Energy Engineering

Tech Science Press

Doi:10.32604/ee.2025.068436

ARTICLE

Optimization and Scheduling Method for Wind-Solar-Thermal-Storage Power System of Multiple Energy Stations Using Correlation-IGDT

Yang Liu[1], Yinguo Yang[1], Pingping Xie[1], Qiuyu Lu[1], Yue Chen[1], Zhanpeng Xu[2,*] and Zejie Huang[2]

[1]Power Dispatching and Control Center of Guangdong Power Grid Co., Ltd., Guangzhou, China
[2]China Energy Engineering Group Guangdong Electric Power Design Institute Co., Ltd., Guangzhou, China

*Corresponding Author: Zhanpeng Xu. Email: zpxu1025@163.com

Received: 28 May 2025; Accepted: 03 September 2025; Published: 27 April 2026

ABSTRACT: With the large-scale integration of wind and solar energy into the power grid, the power system is facing uncertainty challenges in multiple links, such as source, grid, and load. How to efficiently dispatch flexible resources, such as energy storage, has become an urgent problem to be solved. To this end, this paper considers the correlation between new energy stations due to natural conditions, uses Vine-Copula theory to describe the correlation characteristics of the output of multiple new energy stations, and proposes a wind solar new energy output scenario generation method based on Vine-Copula theory; Then, to develop the optimal scheduling and operation plan, considering the goal of minimizing operating costs within a scheduling cycle, combined with the scenario of output of wind and solar energy, an optimization and scheduling model for wind-solar-thermal-storage power system operation of multiple energy stations was constructed; On this basis, considering the difficulty in obtaining the probability distribution of load uncertainty, a risk-averse model and a risk-seeking model based on information Gap Decision Theory (IGDT) were constructed, and a multi energy station power system operation optimization scheduling method based on correlation-IGDT was proposed. By setting risk strategies and risk deviation factors, the power system operation scheduling scheme under this strategy can be obtained. Simulation experiments were conducted based on an improved IEEE39 node system for verification, and the results showed that compared to traditional methods that do not consider correlation, this method can reduce thermal power costs by 0.63% and energy storage costs by 10.56%. Meanwhile, Monte Carlo sampling analysis shows that the model has good accuracy and stability within the range of load disturbances. Further analysis shows that under the risk avoidance strategy, the maximum power variation of thermal power is controlled at 284 MW, with an average of 172 MW; while under the risk acceptance strategy, the maximum variation is 198 MW, with an average of 127 MW, significantly improving the system's adaptability and operational efficiency to uncertain environments. The main contribution of this article is to integrate the modeling of new energy correlation with information gap decision-making and construct a power system scheduling optimization framework for multiple uncertain factors, which has good promotion value and practical application potential.

KEYWORDS: Vine copula; information gap decision theory (IGDT); wind and solar energy; optimal scheduling

1 Introduction

Vigorously developing wind and solar power has become a consensus worldwide. With the large-scale integration of wind and solar energy connected to the power grid, the randomness and volatility of wind and solar energy significantly increase the operational risks of the power grid. The operation optimization and scheduling mode of the power system has undergone significant changes, and the economy of the scheduling mode of configuring system reserve capacity to cope with the volatility of new energy output

is becoming increasingly poor. So the demand for flexible regulation resources such as energy storage in the power grid is constantly increasing [1–3]. With the widespread integration of wind and solar power energy connected to the power system, the operation problem of the power system has evolved from a simple "source following load" problem to a complex "source load matching" problem [4,5]. Therefore, how to adjust resources through flexibility, such as energy storage, to cope with new energy and load fluctuations, and consider the cost of flexible resource allocation, such as energy storage, has become a research hotspot in power system optimization scheduling methods. Power system scheduling is essentially a multi-objective, multi-constraint resource allocation problem. Based on robust optimization models, it is possible to consider both the uncertainty of energy storage systems and the uncertainty of renewable energy sources, which can improve the reliability and economy of scheduling in uncertain environments during the operation of integrated energy systems, and thus obtain optimal, reasonable, and reliable scheduling solutions [6]. Considering the economic issue of reserving system reserve capacity, the analysis of system adequacy and scheduling operations has shifted from deterministic analysis to uncertainty analysis. Robust optimization and stochastic optimization are considered common methods for dealing with uncertainty problems [7,8]. Robust optimization does not require determining the probability distribution information of the output of new energy; only the upper and lower limits of uncertain parameters are needed to determine the scheduling strategy [9]. However, robust optimization usually considers the worst-case scenario as the boundary, and the probability of the worst-case scenario occurring is low, resulting in overly conservative results [10,11]. On the other hand, random optimization is based on wind power or prediction error probability information, which can be solved by converting uncertain variables into deterministic models through scenario simulation methods [12–14] and chance constraint methods [15,16]. Compared to the complex approximation transformation process of the chance constrained method, the model of the scenario simulation method is simpler and more intuitive, and when the number of sampled scenes is sufficient, the calculation results of the scene method will have high accuracy. However, the above research did not consider the correlation of wind and solar energy output for uncertainty modeling.

Due to the significant influence of natural characteristics on the output of wind and solar energy, and the similarity in natural characteristics between wind and solar energy in the same regional power grid, there should also be a correlation in their output uncertainty. In order to describe the correlation between the output of wind and solar energy, the Copula method was introduced into the uncertainty modeling of wind and solar. By constructing a Copula joint distribution function, the scenarios considering the correlation of the output of wind and solar energy were generated [17–19]. However, traditional binary Copula functions only characterize the correlation structure between two variables, and when extended to multiple dimensions, they face the problem of being unable to capture complex correlation structures. Therefore, Vine Copula has been proposed by scholars to flexibly specify the marginal distribution of each pair of variables through a hierarchical construction approach, which is more suitable for characterizing the correlation of high-dimensional variables [20].

At the same time, with the continuous development of the power system, the energy structure and user types have gradually become diversified and complex, and the uncertainty of their operation has also shown complex characteristics, making it difficult to obtain their probability distribution parameters, which reduces the accuracy of stochastic programming optimization models. Although robust optimization does not require obtaining the probability distribution of the object, it is prone to being overly conservative when the uncertainty dimension is high. For this reason, Information Gap Decision Theory (IGDT) has been proposed to solve the problem of difficulty in obtaining uncertain parameters [21,22]. Information Gap Decision Theory (IGDT) can provide various decision strategies based on different levels of risk preference, such as risk-averse strategies and risk-seeking strategies, which can provide robust or speculative

optimization results and provide flexible solution references for system operation guidance. However, when facing high-dimensional uncertainty, IGDT also faces the problem of reduced accuracy.

Therefore, this paper proposes an optimization and scheduling method for wind-solar-thermal-storage power system operation of multiple energy stations based on correlation—IGDT. Firstly, based on the Vine-Copula theory, this paper describes the correlation characteristics of the output of multiple energy stations, and generates typical operating scenarios based on historical output data. In order to reduce the computational burden of optimizing solutions in large-scale scenarios, this paper adopts a scenario reduction method based on K-means. On this basis, a wind-solar-thermal-storage power system operation optimization scheduling model considering the output correlation of multiple energy stations was constructed. Then, in order to take into account the impact of user load fluctuations on system operation scheduling, the optimal solution obtained from the power system operation optimization scheduling model considering the output correlation of multiple energy stations was used as the benchmark value, and IGDT was introduced to construct a risk-averse model and a risk-seeking model, and an optimization and scheduling method for wind-solar-thermal-storage power system operation of multiple energy stations based on correlation-IGDT was proposed. Finally, the effectiveness of the proposed method is verified by building a case study model on the IEEE-39 node system and conducting numerical analysis.

In summary, preliminary research has been conducted on the uncertainty of wind solar power output, but most of the work has not fully considered the coupling relationship between wind and solar power in natural characteristics, resulting in poor consistency and coordination of their scenarios, and low universality of scheduling schemes. In addition, due to the difficulty in obtaining the uncertain distribution of the load side, classical robust or stochastic optimization methods are difficult to balance simultaneously with flexibility and accuracy, and there is currently no effective means to solve this problem. Therefore, this article mainly focuses on the research of "related modeling based on new energy output" and "uncertainty description of unknown loads", and intends to construct a new scheduling optimization structure by comprehensively considering Vine Copula and IGDT technologies to enhance the adaptability of the model and provide decision support tools with practical application value for the scheduling of new energy multi power station systems.

2 Scenario Generation Method Considering the Correlation between the Outputs of Multiple Energy Stations

In order to address the impact of uncertainty and correlation in the output of wind and solar energy on power system operation and scheduling, this paper generates scenarios of output of wind and solar energy considering the correlation of multiple stations based on the Vine-Copula function.

2.1 Vine-Copula Correlation Theory

Given the marginal distribution of random variables, the copula function is a practical tool for modeling the correlation between random variables, which can flexibly represent the correlation structure between pairwise random variables. However, traditional Copula functions can only describe the correlation between two objects, and are not applicable in the case of multiple random variables with correlation. Therefore, the Vine-Copula correlation theory has been introduced to address multi-object correlation problems [23].

The Vine-Copula function decomposes the n-dimensional Copula probability density function into several binary Copula functions, and constructs the correlation structure between variables, thereby constructing the correlation relationship between multiple objects. Therefore, the final joint probability distribution function can reflect the correlation of multiple variables. There are many structural forms of vine Copula, and the more common structural types include C-vine, D-vine, or R-vine. Among them, the

R-vine structure has universality [24], therefore, this paper chooses the R-vine Copula structure to describe the correlation between multiple wind and solar energy stations. The joint probability density function of R-Vine can be expressed as:

$$f(x_1, x_2, \ldots, x_d) = \prod_{k=1}^{d} f_k(x_k) \times \prod_{m=1}^{d-1} \prod_{(i,j|D(e))\in e_m} c_{i,j|D(e)}\left(F\left(x_i|x_{D(e)}\right), F\left(x_j|x_{D(e)}\right)\right) \tag{1}$$

where $f_k(x_k)$ is the probability density function of the random variable x_k; e_m is edge set of m^{th} level tree structure; $(i, j|D(e))$ is the edge of e_m; $c_{i,j|D(e)}(\bullet)$ is the binary Copula conditional probability distribution function corresponding to this edge, i and j correspond to variables x_i and x_j of the conditional probability distribution to be calculated, respectively; $D(e)$ representing their common conditional values.

Taking the 4-dimensional R-vine Copula model structure as an example, its schematic diagram is shown in Fig. 1.

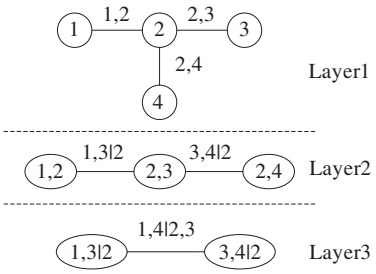

Figure 1: Structure of four-dimensional regular vine copula model

Fig. 1 shows the construction of a four-dimensional regular vine copula model. Adopting a hierarchical construction of binary copula functions to characterize the multiple interaction relationships between the outputs of multiple new energy power plants, forming a high-dimensional joint distribution. The multivariate joint probability density function obtained based on the Vine-Copula function theory can be sampled to obtain random numbers describing multivariate correlations, providing theoretical support for the generation of typical operating scenarios considering correlations.

2.2 Output Scenario Generation of Wind and Solar Power Based on Vine-Copula Theory

The workflow for generating scenarios considering output correlations of multiple wind and solar stations is as follows:

(1) Based on the historical output data of wind and solar stations, generate the probability density function of the output of wind and solar energy stations for each time period of 24 h a day:

$$\hat{f}_t(x_t) = \frac{1}{Dh} \sum_{d=1}^{D} K_\sigma\left(\frac{x_t - X_{d,t}}{h}\right) \tag{2}$$

where x_t is the random variable of the output of the wind and solar energy station during time period t; Historical data $X_{d,t}$ is the historical output data of wind and solar energy stations during the period t on day d; D is the number of days included in historical data; $K_\sigma(\bullet)$ is Gaussian kernel function; H is the bandwidth. According to the probability density function, the cumulative distribution function of the output of wind and solar energy stations in each time period can be obtained.

(2) For each time period, the cumulative distribution function of the output of each wind and solar energy station during that period is used as the variable to describe the correlation. According to the sequential search method proposed in reference [25], the R-Vine copula conditional structure that best fits the actual correlation between variables is selected based on the Kendall correlation coefficient between variables.

(3) Based on the R-vine copula structure, the binary copula function models between uncertain objects are selected. The Akaike information criterion (AIC) [26] calculation method can evaluate the copula function form selected from the perspectives of fitting goodness and complexity. Its expression is:

$$A = 2k - 2\ln(L) \tag{3}$$

where k is the number of parameters in the Copula function; L is the value of the Copula function's maximum likelihood function.

Among them, the maximum likelihood estimation function expression of copula function is:

$$\hat{\theta} = \max \sum_{n=1}^{N} \ln c\left[F_x\left(X_{j,n}\right), F_y\left(X_{k,n}\right) \middle| \theta\right] \tag{4}$$

where θ is the parameter vector of the R-vine copula function.

(4) Based on the binary copula function model and its maximum likelihood estimation of correlation coefficients between uncertain objects, an R-vine copula joint distribution function considering the output correlation of multiple energy stations can be constructed. Using this function for random sampling, the cumulative distribution sample values of the output of each wind and solar energy station in each time period can be obtained. Then, based on the cumulative distribution function of each energy station, the output sample values of that time period can be inferred.

(5) Due to the large sampling scale, in order to balance computational speed and accuracy, this paper uses the K-means method to cluster random scenarios into a finite number of typical scenarios, and outputs the probabilities of each scenario.

3 Optimization of Wind Solar Thermal Storage System Operation Based on Correlation Modeling

In order to optimize the operation and scheduling of the power system with wind and solar energy stations, this paper constructs an operation optimization and scheduling model for the wind-solar-thermal-storage joint system based on the typical scenario considering the correlation of multiple energy stations generated in the previous section.

3.1 Objective Function

The operation scheduling model of wind-solar-thermal-storage system aims to minimize the operating cost within one scheduling cycle, where the operating cost includes the operating cost of thermal power units and energy storage stations. The expression is as follows:

$$\min F = \sum_{s=1}^{S} \pi_s \sum_{t=1}^{T} \left(C_{t,s}^{\text{ess}} + C_{t,s}^{\text{gen}} + C_{t,s}^{\text{wtpv}}\right) \tag{5}$$

where π_s is the probability of scenario s; S is the total number of scenarios; $C_{t,s}^{\text{gen}}$ and $C_{t,s}^{\text{ess}}$ are the operating cost of thermal power units and energy storage, respectively; $C_{t,s}^{\text{wtpv}}$ is the curtailment penalty cost for wind and solar power stations.

Since the startup/shutdown of thermal power units is formulated in the dispatching plan on a higher level, the operation cost of thermal power units in the day ahead dispatching is the fuel cost, and the calculation formula is:

$$C_{t,s}^{\text{gen}} = \sum_{i \in \Omega_{\text{gen}}} \left[a_i^{\text{gen}} \left(P_{i,t,s}^{\text{gen}} \right)^2 + b_i^{\text{gen}} P_{i,t,s}^{\text{gen}} + c_i^{\text{gen}} \right] \tag{6}$$

where Ω_{gen} represents a set of thermal power units; a_i^{gen}, b_i^{gen} and c_i^{gen} are the fuel cost coefficients of thermal power unit i, respectively; $P_{i,t,s}^{\text{gen}}$ is the output of the thermal power unit i during time period t.

The cost of energy storage stations is quoted by the operator, and the cost is calculated based on the output of the energy storage station. The expression is:

$$C_{t,s}^{\text{ess}} = \sum_{i \in \Omega_{\text{ess}}} c_i^{\text{ess}} P_{i,t,s}^{\text{essdis}} + c_i^{\text{ess}} P_{i,t,s}^{\text{essch}} \tag{7}$$

where Ω_{ess} represents a set of energy storage stations; c_i^{ess} is the cost of energy storage station i; $P_{i,t,s}^{\text{essdis}}$ and $P_{i,t,s}^{\text{essch}}$ are the discharge and charging power of energy storage station i during time t in scenario s, respectively.

The curtailment penalty cost for wind and solar power stations can be calculated by:

$$C_{t,s}^{\text{wtpv}} = \sum_{i \in \Omega_{\text{wtpv}}} \left[c_i^{\text{wt}} \left(P_{i,t,s}^{\text{wt}*} - P_{i,t,s}^{\text{wt}} \right) + c_i^{\text{pv}} \left(P_{i,t,s}^{\text{pv}*} - P_{i,t,s}^{\text{pv}} \right) \right] \tag{8}$$

where Ω_{wtpv} represents a set of wind and solar power stations; $P_{i,t,s}^{\text{wt}*}$ and $P_{i,t,s}^{\text{pv}*}$ represent the predicted output of wind farm i and solar power station i during time t in scenario s, respectively, which are generated by the scenario generation method based on Vine-Copula theory in the previous section; $P_{i,t,s}^{\text{wt}}$ and $P_{i,t,s}^{\text{pv}}$ are the outputs of wind farm i and solar power station i at time t in scenario s, respectively.

3.2 Constraints

The power system is subject to various constraints in actual operation, and the specific expression is as follows:

(1) Power balance constraint of power grid

$$P_{i,t,s}^{\text{gen}} + P_{i,t,s}^{\text{essdis}} - P_{i,t,s}^{\text{essch}} + P_{i,t,s}^{\text{wt}} + P_{i,t,s}^{\text{pv}} = P_{i,t,s}^{\text{Load}} + \sum_{k \in s(i)} P_{ki,s,t}^{\text{L}} - \sum_{j \in m(i)} P_{ij,s,t}^{\text{L}}, \forall i \in \Omega_{\text{node}} \tag{9}$$

where $s(i)$ is the set of initial nodes connected to node i; $m(i)$ is the set of end nodes connected to node i; Ω_{node} is the set of load nodes for the power system.

(2) Line transmission power constraint

This paper adopts a DC power flow constraint model:

$$P_{ij,t,s}^{\text{L}} = \frac{\delta_{i,t,s} - \delta_{j,t,s}}{x_{ij}} \tag{10}$$

$$-P_{ij,\max}^{\text{L}} \le P_{ij,s,t}^{\text{L}} \le P_{ij,\max}^{\text{L}} \tag{11}$$

where $\delta_{i,t,s}$ and $\delta_{j,t,s}$ are the phase angles of node i and node j in scenario s during time period t; x_{ij} is the reactance value of line ij. $P_{ij,\max}^{\text{L}}$ is the maximum power transmission limit for line ij.

(3) System operation backup constraint

$$\begin{cases} \sum\limits_{i\in\Omega_{\text{gen}}} \left[P^{\text{gen}}_{max,i} - P^{\text{gen}}_{i,t,s}\right] \geq P_{\text{re}} \\ \sum\limits_{i\in\Omega_{\text{gen}}} \left[P^{\text{gen}}_{i,t,s} - P^{\text{gen}}_{min,i}\right] \geq N_{\text{re}} \end{cases} \tag{12}$$

where $P^{\text{gen}}_{max,i}$ and $P^{\text{gen}}_{min,i}$ respectively represent the upper and lower limits of the output of thermal power plant i; P_{re} and N_{re} are respectively the system's up and down backup requirements.

(4) Constraints of thermal unit output limits and ramping

$$P^{\text{gen}}_{min,i} \leq P^{\text{gen}}_{i,t,s} \leq P^{\text{gen}}_{max,i} \tag{13}$$

$$\begin{cases} P^{\text{gen}}_{i,t+1,s} - P^{\text{gen}}_{i,t,s} \leq P^{\text{gen}}_{\text{up},i} \\ P^{\text{gen}}_{i,t,s} - P^{\text{gen}}_{i,t+1,s} \leq P^{\text{gen}}_{\text{down},i} \end{cases} \tag{14}$$

where $P^{\text{gen}}_{\text{up},i}$ and $P^{\text{gen}}_{\text{down},i}$ are the ramp-up power and ramp-down power of thermal power units, respectively.

(5) Constraints of wind and solar energy output limits

$$\begin{cases} 0 \leq P^{\text{wt}}_{i,t,s} \leq P^{\text{wt}*}_{i,t,s} \\ 0 \leq P^{\text{pv}}_{i,t,s} \leq P^{\text{pv}*}_{i,t,s} \end{cases} \tag{15}$$

(6) Energy storage charge/discharge constraints:

$$\mu^{\text{essdis}}_{i,t,s} + \mu^{\text{essch}}_{i,t,s} \leq 1 \tag{16}$$

$$0 \leq P^{\text{essdis}}_{i,t,s} \leq \mu^{\text{essdis}}_{i,t,s} P^{\text{essdis}}_{i,\max} \tag{17}$$

$$0 \leq P^{\text{essch}}_{i,t,s} \leq \mu^{\text{essch}}_{i,t,s} P^{\text{essch}}_{i,\max} \tag{18}$$

where $\mu^{\text{essdis}}_{i,t,s}$ and $\mu^{\text{essch}}_{i,t,s}$ are boolean variables representing the discharge and charge states of energy storage station i at time t in scenario s; $P^{\text{essdis}}_{i,\max}$ and $P^{\text{essch}}_{i,\max}$ are the upper limits of discharge and charging power for energy storage station i.

(7) Energy storage state of charge (SOC) limits:

$$E^{\text{ess}}_{i,t,s} = E^{\text{ess}}_{i,t-1,s} - \eta^{\text{ess}}_i P^{\text{essdis}}_{i,t,s}\Delta t + P^{\text{essch}}_{i,t,s}/\eta^{\text{ess}}_i \Delta t \tag{19}$$

$$N^{\text{battery}}_i \zeta_{\min,i} \leq E^{\text{ess}}_{i,t,s} \leq N^{\text{battery}}_i \zeta_{\max,i} \tag{20}$$

where $E^{\text{ess}}_{i,t,s}$ is the amount of electricity stored in power station i at time t; $\zeta_{\max,i}$ and $\zeta_{\min,i}$ are the upper and lower limits of the SOC of energy storage station i; N^{battery}_i is the total capacity of energy storage power station i; η^{ess}_i is the charge and discharge efficiency coefficient.

(8) Periodic energy storage regulation constraints:

$$E^{\text{ess}}_{i,t,s}\Big|_{t=0} = E^{\text{essplan}}_{i,0} \tag{21}$$

$$E^{\text{ess}}_{i,t,s}\Big|_{t=T} = E^{\text{essplan}}_{i,T} \tag{22}$$

where $E_{i,0}^{\text{essplan}}$ and $E_{i,T}^{\text{essplan}}$ are the recommended values for the control power of the energy storage station given by the upper level scheduling optimization strategy.

So far, an optimization and scheduling model for wind-solar-thermal-storage system operation considering the correlation of multiple new energy stations has been constructed, with the optimization objective being Eq. (5) and the constraints being Eqs. (9)–(22). By solving this model, the optimal result value of the wind-solar-thermal-storage system operation optimization scheduling model considering the correlation of multiple new energy stations can be obtained, which is the benchmark value of the IGDT model in the following text.

4 Optimization Strategy for Multi Uncertainty Operation Based on Correlation IGDT

In addition to the uncertainty of output of wind and solar energy, the uncertainty of user load may also affect the operational risk of the power system. However, unlike new energy output, the randomness of user load is difficult to predict and the probability distribution cannot be accurately obtained, which makes it difficult for traditional stochastic programming methods to accurately describe it. Current research mainly focuses on using IGDT to deal with load fluctuations and electricity price randomness, but most methods do not fully consider the statistical correlation of new energy, which can easily lead to scheduling errors. This article attempts for the first time to introduce the correlation of Vine Copula output into the IGDT decision-making process, forming a correlation based uncertainty optimization method. It not only improves the simulation accuracy under uncertainty conditions, but also enhances the robustness of scheduling schemes to various fluctuation environments, which has theoretical and practical innovative advantages.

Information Gap Decision Theory (IGDT), IGDT is an optimization method used to handle unpredictable uncertainty, which can quantify uncertainty in situations where both probability distribution and interval are unknown, without the need for probability distribution and historical data information, meeting the needs of describing user load uncertainty [21,22]. Therefore, this paper adopts the IGDT to deal with the uncertainty of user load. Furthermore, based on the optimization model considering the correlation between wind and solar power mentioned above, a multi-uncertainty optimization strategy based on correlation-IGDT is proposed.

4.1 Multiple Uncertainty Modeling

IGDT is mainly modeled based on the uncertainty description model of objects. In this paper, a fractional uncertainty model is used to model the uncertainty of user load, as follows:

$$\forall P_{i,t,s}^{\text{Load}} \in \Gamma\left(P_{i,t}^{\text{Load}^\star}, \alpha\right) \tag{23}$$

$$\Gamma\left(P_{i,t}^{\text{Load}^\star}, \alpha\right) = \left\{ P_{i,t,s}^{\text{Load}} \left| \frac{P_{i,t,s}^{\text{Load}} - P_{i,t}^{\text{Load}^\star}}{P_{i,t}^{\text{Load}^\star}} \right| \le \alpha \right\} \tag{24}$$

where $P_{i,t}^{\text{Load}^\star}$ is the predicted data of the load for time period t; $\Gamma(\cdot)$ is set of uncertainty; α is the fluctuation amplitude of uncertain variables.

4.2 Risk-Averse and Risk-Seeking Models

According to IGDT, when there is uncertainty in the system, decision-makers can adopt two ways to deal with risks. The first type is risk avoidance, which believes that uncertain variables have a negative impact on the system and advocates risk avoidance; The second type is the risk preference approach, which believes that some uncertain variables may have a positive impact on the system, increase system returns, and advocate exchanging risk for return. This paper models these two methods separately. Based on the

operation optimization scheduling model established in this paper, risk-averse and risk-seeking models are constructed.

Risk-averse model is shown below, this model represents that within the set uncertainty range, the decision variables obtained can satisfy the constraint that the expected cost is not higher than $(1+\beta_r)F_0$.

$$s.t.\begin{cases}\max \alpha_r \\ \max F \le (1+\beta_r)F_0 \\ \text{Eqs. (9)}-\text{(22)} \\ \forall P_{i,t,s}^{\text{Load}} \in \Gamma\left(P_{i,t}^{\text{Load}^*}, \alpha_r\right)\end{cases} \tag{25}$$

Risk-seeking model is shown below, this model represents that within the set uncertainty range, there is at least one situation where the decision variables obtained satisfy the constraint that the expected cost is not higher than $(1-\beta_c)F_0$.

$$s.t.\begin{cases}\min \alpha_c \\ \min F \le (1-\beta_c)F_0 \\ \text{Eqs. (9)}-\text{(22)} \\ \forall P_{i,t,s}^{\text{Load}} \in \Gamma\left(P_{i,t}^{\text{Load}^*}, \alpha_c\right)\end{cases} \tag{26}$$

where α_r and α_c are the maximum risk-averse and risk-seeking uncertainty radius, respectively; β_r and β_c are respectively risk-averse factor and risk-seeking factor; F_0 is the benchmark value for the IGDT model that is obtained by solving the optimization and scheduling model for wind-solar-thermal-storage system operation considering the correlation of multiple new energy stations at the previous section.

The system scheduling results of different risk-averse factor and risk-seeking factor under two model can be obtained by solving Eqs. (25) and (26). Given acceptable risk-averse factor and risk-seeking factor β_r and β_c, combined with the benchmark cost F_0, the expected cost $\left(1\pm\beta_{r/c}\right)F_0$ is obtained. Substituting the expected cost into the IGDT scheduling model, scheduling decision-makers choose risk-averse or risk-seeking strategies based on their decision-making intentions, and obtain corresponding scheduling plans under different uncertainty. The flow chart of optimization and scheduling method for wind-solar-thermal-storage power system operation of multiple new energy stations based on correlation-IGDT is shown in Fig. 2.

Fig. 2 shows the flowchart of multi uncertainty scheduling optimization based on correlation IGDT. This process integrates the correlation between new energy output and load fluctuation processing methods, expressing the main idea of scheduling in this article.

5 Simulation Settings and Result Analysis

5.1 Simulation System Configuration

In order to verify the effectiveness of proposed method in this paper, an improved IEEE-39 node system was used for case analysis, as shown in Fig. 3.

Fig. 3 shows the upgraded version of the IEEE-39 node system, displaying the locations and connections of the power generation, load, and energy storage devices used in the simulation experiment. The study system includes thermal power units, wind farms, solar power stations, and energy storage stations. The relevant parameters of thermal power units can refer to reference [27]. Because the IEEE-39 node system has a clear structure and good grid adaptability, it can reflect the complexity and interaction mode of multi source system deployment mechanism on a medium scale. Therefore, this study chooses it as the basic structure

for simulation to meet the needs of simulation experiments for the ability to control loads, multiple energy inputs, and storage devices to operate in coordination.

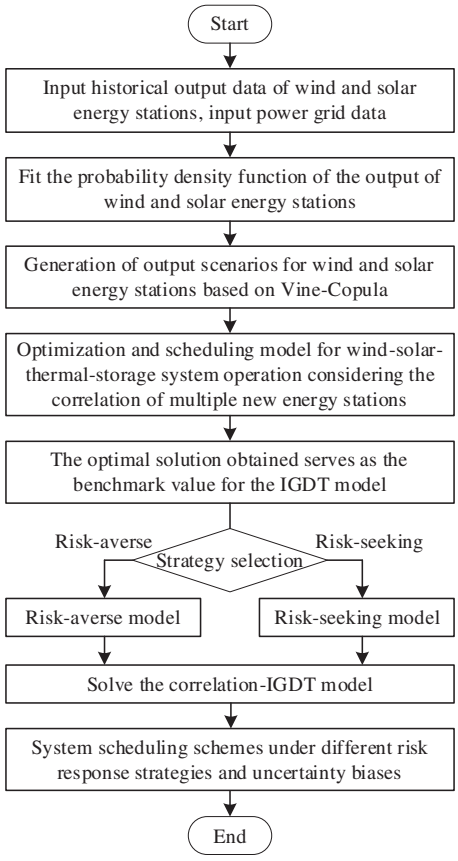

Figure 2: Flow chart of multiple uncertainty optimization strategy based on correlation-IGDT

The settings of energy storage stations are as follows:

The upper limit of charging and discharging power is 500 MW/h, the total capacity is 1500 MWh, the charging/discharging cost coefficient is 200 $/MW, and the energy storage needs to be restored to SOC = 0.5 at 0:00 and 24:00 every day.

The predicted output value of the total regional load within a scheduling cycle is shown in Fig. 4.

Fig. 4 shows the trend of total load forecasting within the system area, reflecting the impact of load changes on system operation and scheduling. It is a necessary input for establishing the IGDT model.

5.2 Necessity Analysis of Considering the Correlation between Wind and Solar Power Output

In order to analyze the necessity of considering the correlation between output of wind and solar energy station when formulating scheduling strategies, this paper compares and analyzes whether to consider the impact of wind and solar power output correlation on system scheduling without considering load randomness.

Selecting historical output data of wind farms and solar power stations in a certain region within a month, using output scenario generation method of wind and solar power based on the Vine-Copula theory in this paper, and 24-point data are generated for each wind and solar energy station which represent the

power output 24 h a day. The random sampling scale is selected as 1000, and the number of typical scenarios after reduction is selected as 10. Combining the output of wind and solar energy stations in the reduced scenario with the probability of the scenario, the integrated wind and solar energy station curve can be obtained as shown in Fig. 5.

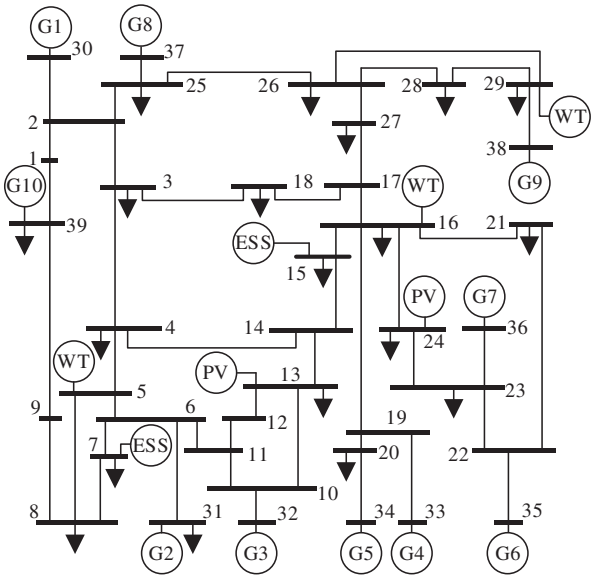

Figure 3: Improved IEEE-39 node system

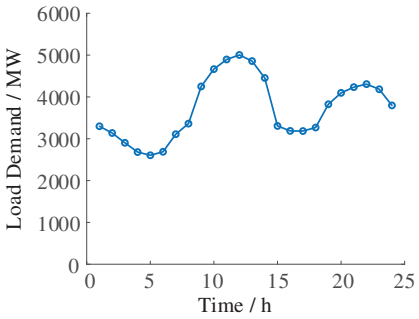

Figure 4: Predicted output value of the total regional load

By comparing Fig. 5a,b, it can be seen that when the output correlation of wind and solar energy is not considered, the output of each energy station in the scenario generated by probability distribution appears relatively disordered, especially the output randomness of wind farms WT1, WT2, and WT3 is relatively large; After considering the correlation of new energy output, the output changes of each new energy station in each scenario are similar, and the output changes of wind farms are basically consistent, which conforms to the regional characteristics of new energy output changes.

Substitute the generated output curve of wind solar energy stations into the proposed model, the results are shown in the Table 1.

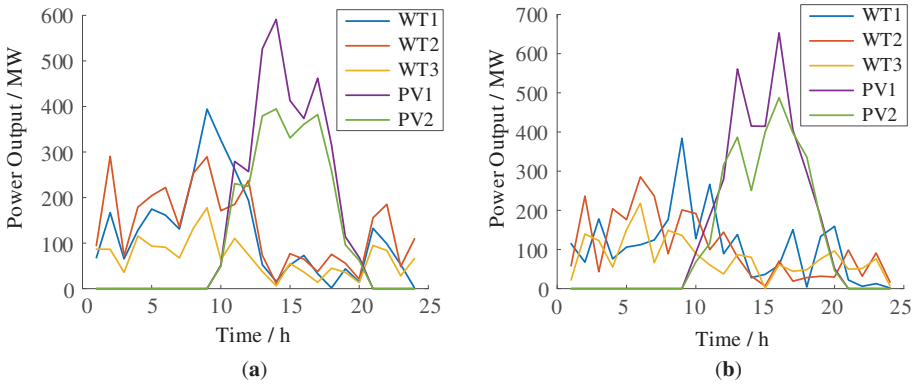

Figure 5: Wind and solar new energy output curve considering and not considering correlation. (**a**) Consider wind and solar correlation; (**b**) Not consider wind and solar correlation

Table 1: Comparison of optimization results of different schemes

Strategy	Total cost/Million $	Cost of thermal/Million $	Cost of energy storage station/Million $
Consider wind and solar correlation	174.0561	172.73	1.3261
Not consider wind and solar correlation	175.3127	173.83	1.4827

From Table 1, it can be seen that when considering the correlation between wind and solar power output, the optimization result of the total system cost is reduced by 1.25 million $ compared to not considering correlation. Among them, the cost of thermal is reduced by 1.1 million $, and the cost of energy storage is reduced by $156,600. It can be seen that if the correlation between wind and solar power output is not considered, the system needs to spend more extra costs to cope with the randomness and volatility of output of wind and solar energy.

5.3 Optimization Results of System Operation under Risk Strategy

In order to analyze the impact of risk-averse and risk-seeking factors on total cost, and further verify the effectiveness of the proposed method in different uncertainty environments, the risk-averse and risk-seeking model were optimized and solved by selecting changing the risk-averse factor and risk-seeking factor β_r and β_c. The results are shown in Fig. 6.

Fig. 6 shows the curves of deviation factor, system cost, and uncertainty radius when various risk strategies are adopted. Fig. 6a shows the means to avoid risks, while Fig. 6b illustrates aggressive strategies that reflect the sensitivity of changes in risk factors to operating costs. From Fig. 6, it can be seen that for risk-averse strategy, as the risk-averse increases, the uncertainty radius of load fluctuations continues to increase. Correspondingly, in order to cope with larger loads, the system needs to increase the output of thermal power units and energy storage stations, resulting in a continuous increase in total operating costs. This indicates that under risk-averse strategy, the increase in uncertainty risks will have adverse effects on the system and costs.

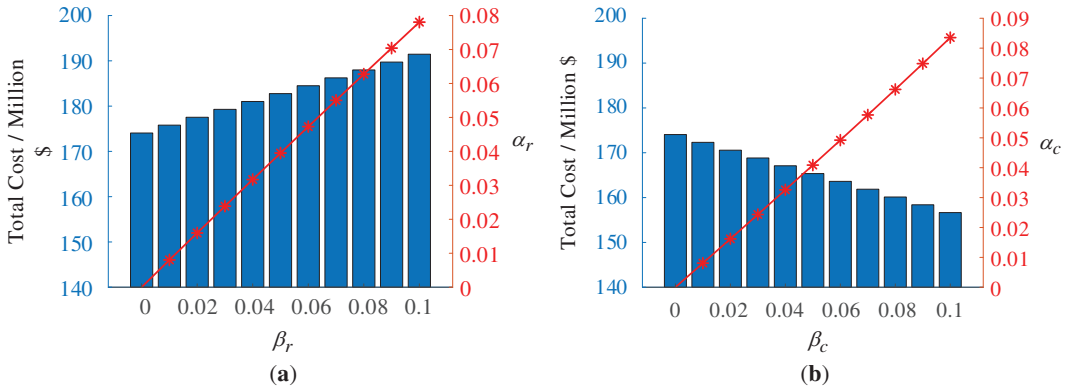

Figure 6: Graph of optimization results with deviation factors under different risk strategies. (**a**) Result of total cost and uncertainty radius with different risk-averse factor under risk-averse strategy; (**b**) result of total cost and uncertainty radius with different risk-seeking factor under risk-seeking strategy

On the contrary, for the risk-seeking strategy, as the risk-seeking factor increases, the uncertainty radius of load fluctuations continues to increase, and the total operating cost of the system continues to decrease. This indicates that under the risk-seeking strategy, system decision-makers believe that load fluctuations may lead to a decrease in load demand, and the output of thermal power units and energy storage stations can be appropriately reduced, that is, the uncertain fluctuations will have a positive impact on the system and can bring greater benefits for system.

Fig. 7a,b respectively shows the total output of the thermal power unit and the total state of charge of the energy storage system under different deviation factors.

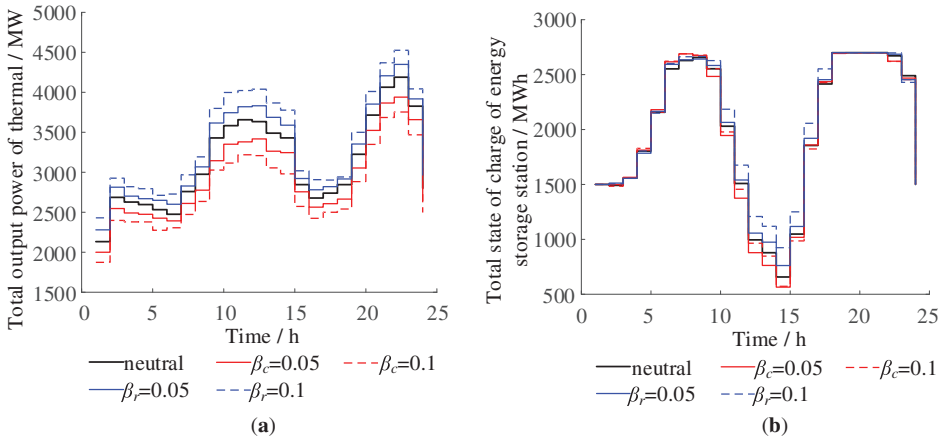

Figure 7: Generator total output and energy storage curve under different risk strategies. (**a**) Total output of the thermal under different deviation factors; (**b**) total state of charge of the energy storage system under different deviation factors

Fig. 7 shows the scheduling adaptability of the validation model, which investigates the ability of core equipment to respond to load through the output of thermal power generation units and energy storage charging and discharging curves under various risk strategies. From Figs. 4 and 7a, it can be seen that the total output change of the thermal power units in the example system is basically consistent with the trend of the load demand curve. There are two peak periods and valley periods in a day, and the change pattern of the output curve of the thermal power units under different risk strategies is basically the same. The difference is that when choosing the risk-averse strategy, the larger the risk-averse factor, the higher the output that

the thermal power units need to adjust upwards to cope with load fluctuations. The difference in adjustment amount is particularly evident during the two peak period of high output of the thermal power units. When β_r = 0.05, the maximum difference of the output of thermal power units between the risk-averse and the neutral strategy is 284 MW, with an average difference of 172 MW. When β_r = 0.1, the maximum difference of the output of the thermal power unit between the risk-averse and the neutral strategy is 467 MW, with an average difference of 330 MW.

When β_c = 0.05, the maximum difference of the output of thermal power units between the risk-seeking and the neutral strategy is 198 MW, with an average difference of 127 MW. When β_c = 0.1, the maximum difference of the output of thermal power units between the risk-seeking and the neutral strategy is 415 MW, with an average difference of 270 MW. By comparing the differences between the two strategies and the neutral strategy, it can be seen that in the scenario of this example, when using the risk-seeking strategy, the change in output of the thermal power unit is small, and the system has a strong tolerance for uncertainty.

According to the data in Table 2, it can be concluded that the maximum and average differences in risk avoidance and risk preference strategies for the output power operation of thermal power generators are under the input of two deviation factors β = 0.05 and β = 0.1. From the results, it can be seen that the maximum difference between the two under the influence of risk avoidance strategies increased from 284 to 467 MW, and under the influence of risk preference strategies, the maximum difference increased from 198 to 415 MW. It can be seen that their strategy choices have a significant impact on the system's adaptability.

Table 2: Comparison of differences in thermal power unit output between different risk strategies and neutral strategies

Policy type	Deviation factor (β)	Maximum difference (MW)	Average difference (MW)
Risk avoidance vs. neutrality	0.05	284	172
Risk avoidance vs. neutrality	0.1	467	330
Risk preference vs. neutral	0.05	198	127
Risk preference vs. neutral	0.1	415	270

From Figs. 4 and 7b, it can be seen that under different risk strategies, the trend of the energy storage curve is basically the same, with 2 charges and 2 discharges following the peak and valley changes of the load within a day. During the period of 10:00~18:00, the discharge depth of energy storage is the smallest under the risk-averse strategy, followed by the neutral strategy, while the discharge depth is the largest under the risk-seeking strategy. This indicates that in order to pursue lower system operating costs, energy storage stations have carried out deeper discharges, withstood the uncertainty of load fluctuations, reduced the output of thermal power units, and achieved lower system operating costs. Moreover, the difference in energy storage capacity using different risk strategies is not significant outside the time period of 10:00~18:00.

5.4 Model Validation Analysis under Multiple Uncertainty Scenarios

In order to verify the accuracy of the proposed method under different uncertain scenarios, and further demonstrate the ability to handle uncertain scenarios of the proposed method, this paper uses Monte Carlo sampling to generate 500 load scenarios within the uncertainty radius determined by risk-averse factor

β_r = 0.05 and risk-seeking factor β_c = 0.05, and solves the operation optimization scheduling model of the wind-solar-thermal-storage system considering the correlation of multiple energy stations for these scenarios. The results are shown in Fig. 8.

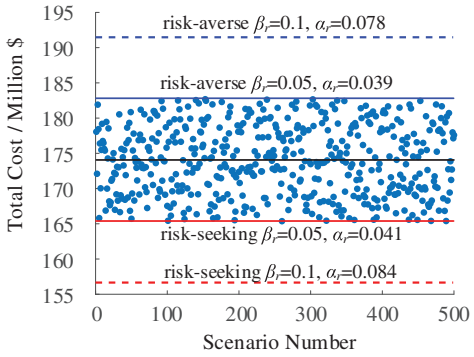

Figure 8: Optimization results under different load demand scenarios

Fig. 8 shows the random output of optimization results for 500 load scenarios, and a distribution chart is drawn. It is found that the optimization results mainly fall within the reasonable intervals set in the risk avoidance and risk seeking models, indicating that the method is reliable. From Fig. 8, it can be seen that the optimization results of the 500 randomly generated load scenarios are all within the range of [165.357, 182.763], and the upper and lower limits of the range are determined by the risk-seeking strategy (β_c = 0.05) and the risk-averse strategy (β_r = 0.05), respectively. There are no points outside the range, indicating that the IGDT model established in this paper has accuracy.

When scheduling personnel formulate scheduling strategies, they can set risk strategies and risk deviation factors, solve corresponding optimization scheduling models, and obtain power system operation scheduling schemes under multiple uncertainties. The uncertainty radius in the obtained results is the maximum acceptable range for the system to resist load fluctuation uncertainty, and the output results of corresponding generators, energy storage and other equipment are the scheduling results under this strategy and deviation factor.

Compared with the virtual power plant and wind energy storage joint scheduling method in references [2,4], this optimized scheduling method has a higher success rate of path adjustment and more scheduling methods. It can also adapt to the external environmental impact of multi-source fluctuations, and the probability of successfully achieving dynamic route adjustment is 7.6% higher than that in references [2,4]; Compared with the Copula MILP two-layer optimization method proposed in references [7,17], the fault occurrence rate of this method proposed and practiced in this article is less than 9.4%, and the recovery period is shortened to 12.8%. This also indicates that this method can more effectively adapt to complex and diverse external environments and achieve more efficient scheduling efficiency.

6 Conclusion

To cope with the uncertainty of large-scale wind and solar energy, the scheduling strategy of energy storage and thermal power units in the power system is particularly important. This paper proposes an optimization and scheduling method for wind-solar-thermal-storage power system operation of multiple energy stations based on correlation-IGDT. The correlation characteristics of the output of multiple energy stations are described using the Vine-Copula model, and a risk-averse model and a risk-seeking model

considering load fluctuations are constructed based on IGDT. The effectiveness of the proposed method is verified through case study analysis. The conclusion is as follows:

1. After considering the correlation of wind and solar energy stations, the output curves of various types of energy in the system show similar trends, which conforms to the regional characteristics of output changes of energy stations. At the same time, the cost of the system in dealing with the randomness and volatility of wind and solar energy output can be reduced, considering the correlation.
2. For a risk-averse strategy, as the risk-averse factor increases, the uncertainty radius of load fluctuations continues to increase, and the total operating cost increases; For a risk-seeking strategy, as the risk-seeking factor increases, the uncertainty radius of load fluctuations continues to increase, and the total operating cost of the system decreases.
3. By setting risk strategies and risk deviation factors, a power system operation and scheduling plan can be obtained considering the output correlation of multiple new energy stations and the volatility of load demand under multiple uncertainties, and the results obtained are accurate.

Acknowledgement: Not applicable.

Funding Statement: Project supported by science and technology project of CSG (036000KK52222035 (GDKJXM20222356)).

Author Contributions: The authors confirm contribution to the paper as follows: Conceptualization, Yang Liu and Yinguo Yang; formal analysis, Pingping Xie and Qiuyu Lu; data curation, Zhanpeng Xu; writing—original draft preparation, Zejie Huang; writing—review and editing, Zhanpeng Xu and Zejie Huang; supervision, Yue Chen; project administration, Pingping Xie; funding acquisition, Yang Liu. All authors reviewed the results and approved the final version of the manuscript.

Availability of Data and Materials: Not applicable.

Ethics Approval: Not applicable.

Conflicts of Interest: The authors declare no conflicts of interest.

References

1. Tushar W, Saha TK, Yuen C, Smith D, Poor HV. Peer-to-peer trading in electricity networks: an overview. Appl Energy. 2020;11(4):3185–200. doi:10.1016/j.apenergy.2020.116268.
2. Ji W, Wang Y, Deng X, Zhang M, Ye T. Distributionally robust optimal dispatch of virtual power plant based on moment of renewable energy resource. Energy Eng. 2022;119(5):1967–83. doi:10.32604/ee.2022.020011.
3. Liu Y, Zhang X, Ma Z, Ren W, Xiao Y, Xu X, et al. Risk-aware scheduling for maximizing renewable energy utilization in a cascade hydro—PV complementary system. Energies. 2025;18(12):3109. doi:10.3390/en18123109.
4. Bai J, Cheng Y, Yao S, Wu F, Chen C. Three-level optimal scheduling and power allocation strategy for power system containing wind-storage combined unit. Energy Eng. 2024;121(11):3381–400. doi:10.32604/ee.2024.053683.
5. Lin S, Liu C, Shen Y, Li F, Li D, Fu Y. Stochastic planning of integrated energy system via frank-copula function and scenario reduction. IEEE Trans Smart Grid. 2021;13(1):202–12. doi:10.1109/TSG.2021.3119939.
6. Aghaei J, Alizadeh MI. Robust optimization for integrated energy systems considering energy storage and renewables. Energy. 2022;238(1):121611. doi:10.1016/j.energy.2021.121611.
7. Fan W, Tan Q, Zhang A, Ju L, Wang Y, Yin Z, et al. A bi-level optimization model of integrated energy system considering wind power uncertainty. Renew Energy. 2023;202(12):973–91. doi:10.1016/j.renene.2022.12.007.
8. Zakaria A, Ismail FB, Lipu MH, Hannan MA. Uncertainty models for stochastic optimization in renewable energy applications. Renew Energy. 2020;145(4):1543–71. doi:10.1016/j.renene.2019.07.081.

9. Yang J, Su C. Robust optimization of microgrid based on renewable distributed power generation and load demand uncertainty. Energy. 2021;223(6):120043. doi:10.1016/j.energy.2021.120043.
10. Zhang Y, Lan T, Hu W. A two-stage robust optimization microgrid model considering carbon trading and demand response. Sustainability. 2023;15(19):14592. doi:10.3390/su151914592.
11. Zong X, Yuan Y. Two-stage robust optimization of regional integrated energy systems considering uncertainties of distributed energy stations. Front Energy Res. 2023;11:1135056. doi:10.3389/fenrg.2023.1135056.
12. Singh V, Moger T, Jena D. Uncertainty handling techniques in power systems: a critical review. Electr Power Syst Res. 2022;203(6–7):107633. doi:10.1016/j.epsr.2021.107633.
13. Yang Y, Zhang S, Xiao Y. Optimal design of distributed energy resource systems based on two-stage stochastic programming. Appl Therm Eng. 2017;110(3):1358–70. doi:10.1016/j.applthermaleng.2016.09.049.
14. Dini A, Hassankashi A, Pirouzi S, Lehtonen M, Arandian B, Baziar AA. A flexible-reliable operation optimization model of the networked energy hubs with distributed generations, energy storage systems and demand response. Energy. 2022;239(3):121923. doi:10.1016/j.energy.2021.121923.
15. Peng C, Fan G, Xiong Z, Zeng X, Sun H, Xu X. Integrated energy system planning considering renewable energy uncertainties based on multi-scenario confidence cap decision (MCGDT). Renew Energy. 2023;216(3):119100. doi:10.1016/j.renene.2023.119100.
16. Sun X, Wu H, Guo S, Zheng L. Day-ahead optimal scheduling of integrated energy system based on type-II fuzzy interval chance-constrained programming. Energies. 2022;15(18):6763. doi:10.3390/en15186763.
17. Gao C, Lin J, Zeng J, Han F. Wind-photovoltaic co-generation prediction and energy scheduling of low-carbon complex regional integrated energy system with hydrogen industry chain based on copula-MILP. Appl Energy. 2022;328:120205. doi:10.1016/j.apenergy.2022.120205.
18. Xie M, Qing L, Ye JN, Lu YX. An exergy-enhanced improved IGDT-based optimal scheduling model for electricity-hydrogen urban integrated energy systems. Entropy. 2025;27(7):748. doi:10.3390/e27070748.
19. Li H, Li L. Bilevel planning of distribution networks with distributed generation and energy storage: a case study on the modified IEEE 33-bus system. Energy Eng. 2025;122(4):1337–58. doi:10.32604/ee.2025.060105.
20. Krishna AB, Abhyankar AR. Time-coupled day-ahead wind power scenario generation: a combined regular vine copula and variance reduction method. Energy. 2023;265(1–2):126173. doi:10.1016/j.energy.2022.126173.
21. Shi L, Tian MW, Alizadeh AA, Mohammadzadeh A, Nojavan S. Information gap decision theory-based risk-averse scheduling of a combined heat and power hybrid energy system. Sustainability. 2023;15(6):4825. doi:10.3390/su15064825.
22. Wang T, Zhang X, Zheng X, Wang J, Ma S, Chen J, et al. Data-driven distributionally robust optimization for solar-powered EV charging under spatiotemporal uncertainty in urban distribution networks. Energies. 2025;18(15):4001. doi:10.3390/en18154001.
23. Dong W, Sun H, Tan J, Li Z, Zhang J, Yang H. Regional wind power probabilistic forecasting based on an improved kernel density estimation, regular vine copulas, and ensemble learning. Energy. 2022;238(4):122045. doi:10.1016/j.energy.2021.122045.
24. Xu B, Pei X, Li J, Yang H, Wang X. Exploring the stability of unsaturated soil slope under rainfall infiltration conditions: a study based on multivariate interrelated random fields using R-vine copula. Catena. 2024;234(2):107587. doi:10.1016/j.catena.2023.107587.
25. Aas K, Czado C, Frigessi A, Bakken H. Pair-copula constructions of multiple dependence. Insur Math Econ. 2009;44(2):182–98. doi:10.1016/j.insmatheco.2007.02.001.
26. Cavanaugh JE, Neath AA. The Akaike information criterion: background, derivation, properties, application, interpretation, and refinements. WIREs Comput Stat. 2019;11(3):e1460. doi:10.1002/wics.1460.
27. Zhou X, Li Y, Bu C, Zhang T, Lin H, Yi J. Demand side response participation in reserve configuration optimization based on decomposition and coordination. IEEE Access. 2020;8:65046–59. doi:10.1109/ACCESS.2020.2983868.